Chemical Physics 120 (1988) 261–271
North-Holland, Amsterdam

SEMICLASSICAL WAVE PACKET DYNAMICS IN NONADIABATIC PROCESSES: THE CONICAL INTERSECTION BETWEEN THE $\tilde{X}$ AND $\tilde{A}$ STATES OF $C_2H_4^+$

D. DEHARENG

Département de Chimie, Université de Liège, Sart-Tilman, B-4000 Liège 1, Belgium

Received 29 June 1987; in final form 9 November 1987

Autocorrelation and probability functions are calculated by semiclassical wave packet dynamics for the nuclear evolution of $C_2H_4^+$ in its $\tilde{A}$ state, connected with the $\tilde{X}$ state via conical intersection. Three distinct choices of potential energy surfaces were made: the canonic diabatic surface H_{22}, as defined by Köppel, the adiabatic surface E_2 and the Nikitin diabatic one $\overline{H}_{22}$. The wave packet is expanded in a Gaussian basis set restricted to 40 functions. The influence of the initial Gaussian width as well as the influence of freezing this width or not is studied. Taking into account the fact that the basis set is very small, one can conclude that the results are in acceptable qualitative agreement with those obtained by Köppel. The apparent discrepancy between the canonic diabatic autocorrelation function and the exact one could be explained by the existence of a dynamical condition for the choice of the diabatic potential energy surface. In the case of $C_2H_4^+(\tilde{A})$, the behavior during the relaxation cannot be considered as essentially diabatic or adiabatic: it is intermediate.

1. Introduction

Semiclassical wave packet dynamics (WPD) is nowadays a widely used technique to investigate the chemical reactivity and has already proven its usefulness in the study of scattering or photodissociation problems [1–3] or nonadiabatic processes [4], in the calculation of spectra [5] or the determination of the vibrational states of molecules [6,7]. Furthermore, nonadiabatic processes are important relaxation phenomena in polyatomic molecules and their study is enjoying growing popularity [4,8,9].

The purpose of this work is to study by WPD the short-time dynamical behavior of the nonadiabatic process resulting from the conical intersection between the $\tilde{A}$ and $\tilde{X}$ states of $C_2H_4^+$. The spectrum and the autocorrelation function have already been determined for model potentials [9,10] and it seemed interesting to try to explain, on a dynamical point of view, the apparent adiabatic/diabatic disparity that the authors obtained between their exact autocorrelation function and the diabatic one. Section 2 briefly describes the general framework of this study. In section 3, we present the potential energy surfaces used to run the classical trajectories and section 4 is devoted to the choice of their initial conditions. Section 5 deals with the two Gaussian basis sets used which differ in the fact that one is frozen and the other is not. The equations of motion constitute the little section 6. Section 7 and section 8 present respectively the 3D analytical formula used to calculate the transition probability and the general expressions for the autocorrelation function $C(t)$ and for the global probability $\Pi(t)$ of remaining on the investigated potential energy surface. Section 9 deals with the results that were obtained and section 10 is devoted to their discussion and interpretation.

2. General framework

Why does not the diabatic correlation function obtained by Köppel match at least one part of the exact correlation function? In order to answer this question, one will study the dynamical behavior of the $C_2H_4^+$ ion in a time range where the following approximation is more or less valid: the correlation function has mainly two components, one

0301-0104/88/$03.50

purely adiabatic, the other purely diabatic, and the interference terms are negligible. By interference terms one refers to those trajectories which follow the adiabatic surface for one moment, then jump to the diabatic surface for a certain time, thus moving back and forth on both surfaces. The approximation

$$C(t) \approx C^{\mathrm{ad}}(t) + C^{\mathrm{d}}(t) \tag{2.1}$$

is more or less valid till after the first adiabatic and diabatic recurrences, i.e. $t \approx 1000$ au (see later). In the equation (2.1) there is a problem of normalization, i.e. $C^{\mathrm{ad}}(t)$ and $C^{\mathrm{d}}(t)$ are calculated and normalized separately and $C(t)$ must then be renormalized. The problem arises from the fact that for $t = 0$ and the very initial motion, the adiabatic and diabatic wave packets are quite similar because they move on the same surfaces. As a consequence, the correlation function from $t = 0$ to the coupling region should be the average of $C^{\mathrm{ad}}(t)$ and $C^{\mathrm{d}}(t)$. However, as soon as the interaction region is reached, one can consider that the two wave packets are really complementary because the probability of remaining on the investigated surface (see section 5) is taken into account and then (2.1) holds without normalization.

3. Potential energy surfaces

The potential energy surfaces used in this study are derived from the analytical diabatic model surfaces of Köppel [10]:

$$H_{jj} = E_j^0 + \sum_{i=1}^{2} \left[\tfrac{1}{2}\hbar\omega_{i\mathrm{g}}\left(Q_{i\mathrm{g}}^2 - 1\right) + \sqrt{2}\,\kappa_i(j) Q_{i\mathrm{g}} \right] + \tfrac{1}{2}\hbar\omega_{\mathrm{u}}\left(Q_{\mathrm{u}}^2 - 1\right), \quad j = 1, 2, \tag{3.1}$$

$$H_{ij} = \sqrt{2}\,\lambda Q_{\mathrm{u}}. \tag{3.2}$$

$Q_{i\mathrm{g}}$ are two totally symmetric dimensionless coordinates (corresponding to the C–H and C–C stretching modes ν_1 and ν_2) and Q_{u} is an antisymmetric one (corresponding to the torsional mode ν_4), E_j^0 are the vertical ionisation energies of the two states $|1\rangle$ and $|2\rangle$ and $\omega_{1\mathrm{g}}$, $\omega_{2\mathrm{g}}$, ω_{u} are the frequencies of the three modes and are taken equal in the two states. $\kappa_i(j)$ are called the intrastate coupling constants and λ the interstate coupling one. Their values are given in ref. [10].

Three distinct pairs of potential energy surfaces were considered. The first one is the pair of diabatic surfaces H_{jj} as defined above and which we shall name the "canonic" diabatic surfaces in the following. The second pair are the two adiabatic surfaces E_j obtained by diagonalizing the matrix **H**. The third pair $\overline{H}_{jj}$ is obtained by rotating the matrix **H**. The angle of rotation is determined for each of the N trajectories $(\boldsymbol{Q}_k(t), \boldsymbol{P}_k(t))$ (see section 5) so that the initial potential energy $\overline{H}_{22}(\boldsymbol{Q}_k(0))$ is equal to the adiabatic energy $E_2(\boldsymbol{Q}_k(0))$. These N conditions ensure that the initial wave packet begins to move in a region where the coupling is negligible so that the diabatic surfaces coincide with the adiabatic ones. In the text, these diabatic surfaces $\overline{H}_{jj}$ will be called the "Nikitin" diabatic surfaces [8].

4. Initial conditions

The initial absolute values of the coordinates $(Q_{i\mathrm{g}}, Q_{\mathrm{u}})$ and their conjugate momenta $(P_{i\mathrm{g}}, P_{\mathrm{u}})$ are chosen according to the values of the Wigner function [11]. Two thousand values of $W(Q_{i\mathrm{g}}, Q_{\mathrm{u}}, P_{i\mathrm{g}}, P_{\mathrm{u}})$ are randomly generated and the N sets $(Q_{i\mathrm{g}}, Q_{\mathrm{u}}, P_{i\mathrm{g}}, P_{\mathrm{u}})$ used as initial conditions correspond to the N highest values of W. The signs of the coordinates and momenta are not chosen at random as was already done in another study [4] but rather in the following way. In the first step, they are generated randomly and a control is done as whether the algebraic values of $(Q_{i\mathrm{g}}, Q_{\mathrm{u}}, P_{i\mathrm{g}}, P_{\mathrm{u}})$ really describe a Gaussian distribution for the initial wave packet since it represents the fundamental vibrational wave packet of the molecule. This was not the case because only 10, 20 or 40 initial conditions were retained. The signs were then changed to simulate as well as possible a Gaussian wave packet more or less symmetrically dispersed around $Q_{i\mathrm{g}} = Q_{\mathrm{u}} = 0$.

5. The Gaussian basic sets

A variety of approaches exists for solving the time-dependent Schrödinger equation: among these, the complete numerical integration of the initial wave packet [12] or the expansion of this wave packet on a complete basis set. For example, one can expand it on orthogonal basis functions (like harmonic oscillator eigenfunctions [13]) or on a set of Gaussian basis functions [4,14,15]. This work is constructed on the latter scheme: the (a)diabatic wavefunction is written:

$$\Psi(\boldsymbol{Q}, t) = \sum_k c_k G_k(\boldsymbol{Q}, \boldsymbol{Q}_k, \boldsymbol{P}_k, t)\sqrt{\mathscr{P}_k(t)}\,. \quad (5.1)$$

$\mathscr{P}_k$ is the probability of remaining on the (a)diabatic surface considered,

$$G_k(\boldsymbol{Q}, \boldsymbol{Q}_k, \boldsymbol{P}_k, t) = \exp\Big\{-\tfrac{1}{2}[\boldsymbol{Q}-\boldsymbol{Q}_k(t)]^{\mathrm{T}}\cdot\mathbf{B}_k[\boldsymbol{Q}-\boldsymbol{Q}_k(t)] + \mathrm{i}\hbar^{-1}\boldsymbol{P}_k^{\mathrm{T}}(t)\cdot[\boldsymbol{Q}-\boldsymbol{Q}_k(t)] + \mathrm{i}\hbar^{-1}\gamma_k(t)\Big\}, \quad (5.2)$$

where $\boldsymbol{Q}$ represents the vector (Q_{ig}, Q_u), $[\boldsymbol{Q}_k, \boldsymbol{P}_k]$ is the center of G_k, $\mathbf{B}_k$ is a time-dependent complex 3×3 matrix, and γ_k is a phase term. As a matter of fact, in the expression (5.1) of $\Psi(\boldsymbol{Q}, t)$, the Gaussians should have been multiplied by probability amplitudes. However, one has to be careful about the way to calculate them. For instance, if one wants to use the well-known "classical trajectory amplitudes" [8]

$$\dot{a}_j(t) = -\mathrm{i}\hbar^{-1}\sum_{m\neq j} a_m(t)\Big(H_{jm}^{\mathrm{el}} - \mathrm{i}\hbar\dot{\boldsymbol{Q}}\cdot\boldsymbol{g}_{j\mathrm{m}}\Big) \times\exp\Big(-\mathrm{i}\hbar^{-1}\int_0^t\Big(H_{mm}^{\mathrm{el}} - H_{jj}^{\mathrm{el}}\Big)\,\mathrm{d}t'\Big)$$

one has to reformulate them because a part of the phase factor is already taken into account into the γ_k phase term. Thus, one finally chose to work with a simplified model where the probability amplitudes are merely replaced by the square root of the probability.

For the sake of readability , $G_k(\boldsymbol{Q}, \boldsymbol{Q}_k, \boldsymbol{P}_k, t)$ will be written $G_k(\boldsymbol{Q}, t)$ in the following. The initial matrices $\mathbf{B}_k^0$ are chosen diagonal (this can be justified by the orthogonality of the coordinates), real and independent on k:

$$\mathbf{B}_k^0 = \begin{pmatrix} b & 0 & 0 \\ 0 & b & 0 \\ 0 & 0 & b \end{pmatrix}, \quad (5.3)$$

where two values of b have been used: $b = 1, 2$.

In reality, the wavefunction represented by the relations (5.1) and (5.2) does not obey the unitarity criterion [16]:

$$\langle\Psi(t)\,|\,\Psi(t)\rangle = |\,\Psi_0\,|^2 \quad (5.4)$$

and this for two reasons. The first one is the presence of $\sqrt{\mathscr{P}_k(t)}$, i.e. the fact that one only considers a partial wavefunction. The second reason is the absence of the time-dependent prefactor [16]:

$$\mathscr{B}(\boldsymbol{Q}_k, \boldsymbol{P}_k, t) = \left|\frac{1}{2}\left(\frac{\partial\boldsymbol{P}_k(t)}{\partial\boldsymbol{P}_k(0)} + \frac{\partial\boldsymbol{Q}_k(t)}{\partial\boldsymbol{Q}_k(0)} - 2\mathrm{i}\gamma\hbar\frac{\partial\boldsymbol{Q}_k(t)}{\partial\boldsymbol{P}_k(0)} + \frac{\mathrm{i}}{2\gamma\hbar}\frac{\partial\boldsymbol{P}_k(t)}{\partial\boldsymbol{Q}_k(0)}\right)\right|^{1/2}. \quad (5.5)$$

The absence of $\mathscr{B}(\boldsymbol{Q}_k, \boldsymbol{P}_k, t)$ in (5.1) will be taken into account in two steps: firstly, by renormalizing $\Psi(t)$ by a time-dependent factor $\mathscr{N}(t)$:

$$\mathscr{N}(t) = \Big(\sum_j\sum_k c_j^* c_k S_{jk}(t)\Big)^{1/2}, \quad (5.6)$$

and secondly, by evaluating the c_k at each time step (see below).

Furthermore, the Gaussian functions are not orthogonal. In order to determine properly the coefficients c_k, one has to diagonalize the basis to control the degree of redundancy [4,6]. The determination of the coefficients c_k depends on the potential energy surface on which the nuclear motion takes place and on the choice of b (see eq. (5.3)). If b is equal to 1 (this Gaussian width matches the frequency associated with that of the initial state), and if the motion takes place on the canonic diabatic energy surface (which is harmonic), the matrix $\mathbf{B}_k(t)$ remains constant (see section 6). Thus, the N coefficients c_k are determined once for all from the $P \leqslant N$ linearly independent orthogonal basis functions $F_j(\boldsymbol{Q}, 0)$

[4] obtained by diagonalization of $S_{jk}(0)$:

$$\Psi(\boldsymbol{Q}, 0) = \sum_{j}^{P} u_j F_j(\boldsymbol{Q}, 0) = \sum_{k}^{N} c_k G_k(\boldsymbol{Q}, 0), \quad (5.7)$$

$$F_j(\boldsymbol{Q}, 0) = \sum_{m}^{N} f_{jm} G_m(\boldsymbol{Q}, 0). \quad (5.8)$$

This is also the case in the frozen Gaussian approximation [14] where the $\mathbf{B}_k(t)$ are maintained constant. However, this is no longer true if the $\mathbf{B}_k(t)$ are allowed to vary according to the Schrödinger equation (see section 6) and if either $b \neq 1$ or the potential energy surface is not the canonic diabatic one. Thus, the coefficients u_j and c_k are evaluated at each time step (see appendix) and will be written $c_k^{(t)}$ in the text.

6. Equations of motion

They are derived from the time-dependent Schrödinger equation for each Gaussian function:

$$\mathrm{i}\hbar \frac{\partial G_k(\boldsymbol{Q}, t)}{\partial t} = \hat{H} G_k(\boldsymbol{Q}, t). \quad (6.1)$$

Let us drop the index k and decompose the complex matrix $\mathbf{B}$ and the phase term γ into their real and imaginary parts:

$$\mathbf{B} = \mathbf{B}^{(\mathrm{r})} + \mathrm{i}\mathbf{B}^{(\mathrm{i})}, \quad (6.2)$$

$$\gamma = \gamma^{(\mathrm{r})} + \mathrm{i}\gamma^{(\mathrm{i})}. \quad (6.3)$$

Thus,

$$\dot{B}_{mn}^{(\mathrm{r})} = \sum_j \omega_j \left(B_{jn}^{(\mathrm{r})} B_{jm}^{(\mathrm{i})} + B_{jm}^{(\mathrm{r})} B_{jn}^{(\mathrm{i})} \right), \quad (6.4)$$

$$\dot{B}_{mn}^{(\mathrm{i})} = \sum_j \omega_j \left(B_{jn}^{(\mathrm{i})} B_{jm}^{(\mathrm{i})} - B_{jn}^{(\mathrm{r})} B_{jm}^{(\mathrm{r})} \right) + \hbar^{-1} \frac{\partial^2 V}{\partial Q_n \partial Q_m}, \quad j, n, m = 1, 2, 3, \quad (6.5)$$

$$\dot{Q}_j = \omega_j \hbar^{-1} P_j, \quad (6.6)$$

$$\dot{P}_j = -\frac{\partial V}{\partial Q_j}, \quad (6.7)$$

$$\dot{\gamma}^{(\mathrm{r})} = \tfrac{1}{2} \sum_j P_j \dot{Q}_j - \tfrac{1}{2}\hbar \sum_j \omega_j B_{jj}^{(\mathrm{r})} - V(\boldsymbol{Q}(t)), \quad (6.8)$$

$$\dot{\gamma}^{(\mathrm{i})} = -\tfrac{1}{2}\hbar \sum_j \omega_j B_{jj}^{(\mathrm{i})}, \quad (6.9)$$

$$j = 1, 2, 3,$$

where $V(\boldsymbol{Q}(t))$ is the value, at the center $\boldsymbol{Q}(t)$ of the Gaussian, of the potential (adiabatic or diabatic) on which the Gaussian wave packet moves.

These equations are numerically integrated by the Adams–Moulton–Bashforth algorithm [17]. The numerical integration of the nonlinear equations (6.4) and (6.5) may be subject to some difficulties if the initial values of the B_{mn} are too big. For instance, in this case of $C_2H_4^+(\tilde{A}/\tilde{X})$, $b = 3$ (see eq. (5.3)) seems to be a limit, i.e. some problems arise for a few trajectories. Then, the integration of Heller's $\mathbf{P}_Z$ and $\mathbf{Z}$ matrices [2] seems more appropriate when numerical difficulties are encountered.

7. The transition probability

The formula used to determine the transition probability is obtained in a way similar to that used by Nikitin to derive its two-dimensional expression [8], extended to a linear trajectory characterized by the three coordinates (Q_{1g}, Q_{2g}, Q_u). One obtains the probability p of remaining on the same diabatic state:

$$p = \exp\left(-\frac{4\pi\lambda^2}{\hbar} \times \frac{\left[\dot{Q}_u K_u - Q_u \left(K_{1g}\dot{Q}_{1g} + K_{2g}\dot{Q}_{2g} \right) \right]^2}{\left[\left(K_{1g}\dot{Q}_{1g} + K_{2g}\dot{Q}_{2g} \right)^2 + 8\lambda^2 \dot{Q}_u^2 \right]^{3/2}} \right), \quad (7.1)$$

where

$$K_{ig} = \sqrt{2}\left[\kappa_i(2) - \kappa_i(1) \right], \quad (7.2)$$

$$K_u = \sum_{i=1}^{2} K_{ig} \left(Q_{ig} - Q_{ig}^0 \right), \quad (7.3)$$

$$Q_{ig}^0 = (-1)^{i-1} \frac{E_i^0}{K_{ig}}. \quad (7.4)$$

Each Gaussian G_k is propagated on the potential surface considered and every time its center passes through the seam $H_{22} - H_{11} = 0$, one calculates

$p_k(t)$ by (7.1). At that moment, K_u is equal to zero and Q_u plays the role of an impact parameter to the apex of the conical intersection [4]. The final probability of remaining on the diabatic surface for G_k at time t is given by:

$$\mathscr{P}_k^{\mathrm{d}}(t) = \prod_{j=1}^{n_k(t)} p_k(t_j), \tag{7.5}$$

and the final probability of remaining on the adiabatic surface is given by:

$$\mathscr{P}_k^{\mathrm{ad}}(t) = \prod_{j=1}^{n_k(t)} \left[1 - p_k(t_j)\right], \tag{7.6}$$

where $n_k(t)$ represents the number of passages through the seam at time t, and t_j denotes the value of t for the jth crossing.

8. The correlation function and the global probability

As has been pointed out in section 5, the wavefunction is normalized at each time step:

$$\Psi(\boldsymbol{Q}, t) = \frac{1}{\mathscr{N}(t)} \sum_k c_k^{(t)} \sqrt{\mathscr{P}_k(t)}\, G_k(\boldsymbol{Q}, t), \tag{8.1}$$

where

$$\mathscr{N}(t) = \left(\sum_j \sum_k c_j^{*(t)} c_k^{(t)} S_{jk}(t) \right)^{1/2}. \tag{8.2}$$

The correlation function $C(t)$ and the global probability $\Pi(t)$ of remaining on the investigated potential surface are written:

$$C(t) = \frac{1}{\mathscr{N}(t)} \sum_j \sum_k c_j^{*(0)} c_k^{(t)} \sqrt{\mathscr{P}_k(t)} \times \int \mathrm{d}\boldsymbol{Q}\, G_j^*(\boldsymbol{Q}, 0) G_k(\boldsymbol{Q}, t), \tag{8.3}$$

$$\Pi(t) = |\mathscr{N}(t)|^{-2} \sum_j \sum_k c_j^{*(t)} c_k^{(t)} \times \sqrt{\mathscr{P}_j(t) \mathscr{P}_k(t)}\, S_{jk}(t). \tag{8.4}$$

9. Results

All the calculations were done with $N = 40$ Gaussian functions. This number corresponds to a minimum of basis functions below which the result is much too dependent on N, as tests with $N = 10$ and $N = 20$ showed. This minimum number is a function of the initial value b (see eq. (5.3)) [18].

Four series of calculations were performed which differ by the initial value b ($b = 1$ or 2) and by the fact that **B** is or is not held frozen during the evolution of the Gaussians.

9.1. Influence of b

9.1.1. **B** is allowed to vary

The recurrences of $C(t)$ are higher for $b = 2$ and the relative intensities are different (see fig. 1).

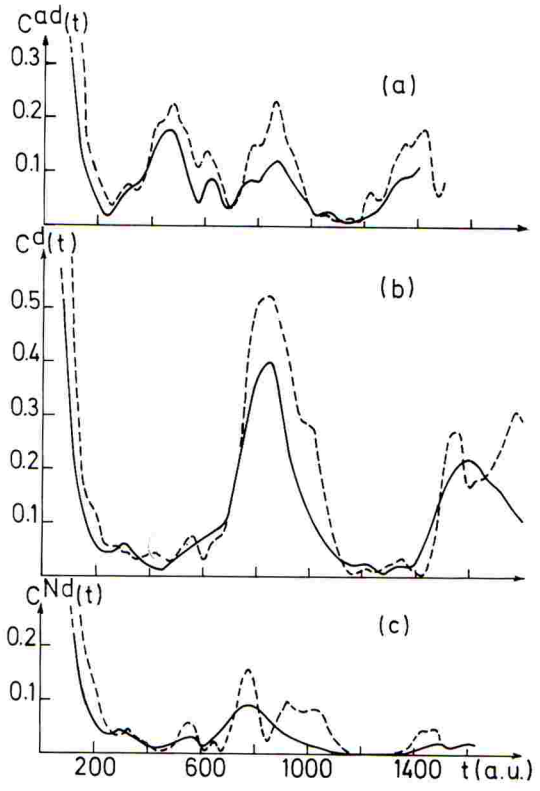

Fig. 1. Autocorrelation functions calculated with the $\mathbf{B}_k$ matrices which vary as a function of time. Full line: $b = 1$; dashed lines: $b = 2$. (a) $C^{\mathrm{ad}}(t)$; (b) $C^{\mathrm{d}}(t)$; (c) $C^{\mathrm{Nd}}(t)$.

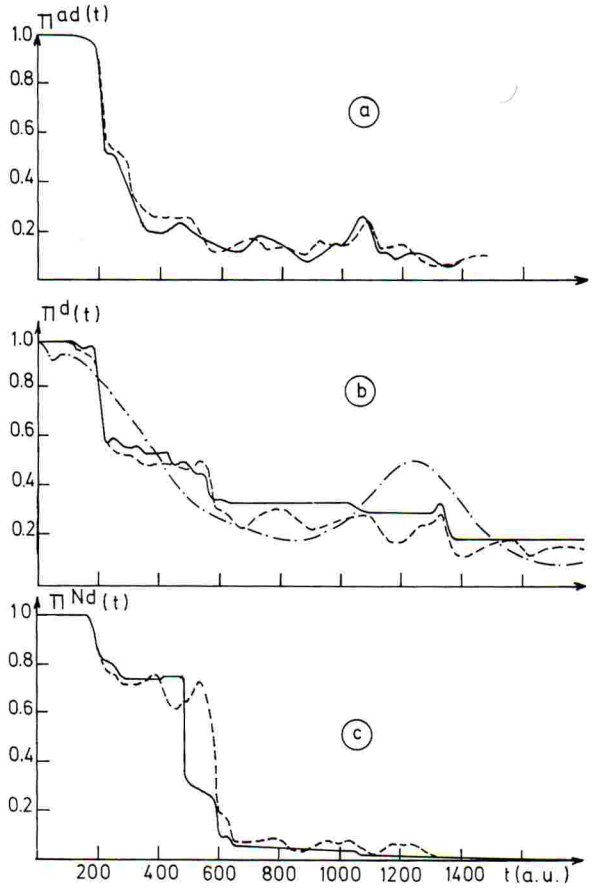

Fig. 2. Probability functions of remaining on the potential energy surface studied as a function of time, calculated with the $\mathbf{B}_k$ matrices which vary with time. Full line: $b = 1$; dashed line: $b = 2$. (a) $\Pi^{ad}(t)$; (b) $\Pi^{d}(t)$ – dash-dotted line: Köppel's $P_2(t)$; (c) $\Pi^{Nd}(t)$.

As far as the canonic diabatic state is concerned, the second recurrence is split into two components when $b = 2$ (fig. 1b). Furthermore, in the case of the Nikitin diabatic state (fig. 1c), a recurrence appears for $b = 2$ at $t \approx 1000$ au which is absent for $b = 1$.

The probabilities $\Pi(t)$ are rather similar except that, in the canonic diabatic case, the oscillatory behavior is more pronounced for $b = 2$ (see fig. 2).

*9.1.2. **B** is frozen*

The comparison is made only between the motions of the wave packet on the adiabatic and the Nikitin diabatic surfaces. As it can be seen from

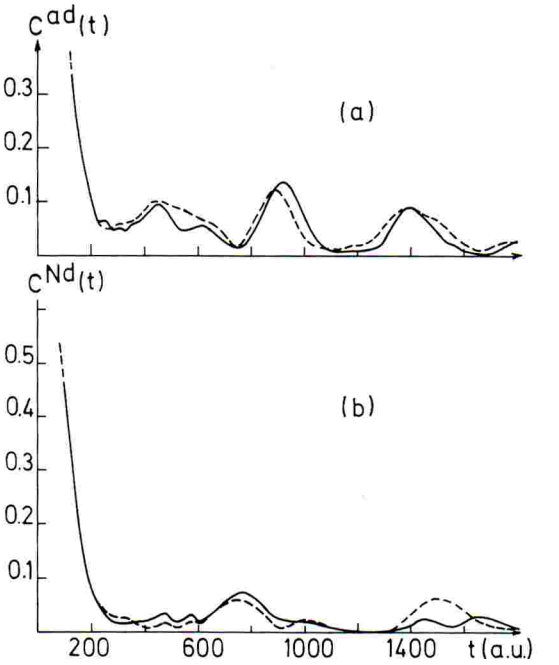

Fig. 3. Autocorrelation functions calculated with frozen $\mathbf{B}_k$ matrices. Full line: $b = 1$; dashed line: $b = 2$. (a) $C^{ad}(t)$; (b) $C^{Nd}(t)$.

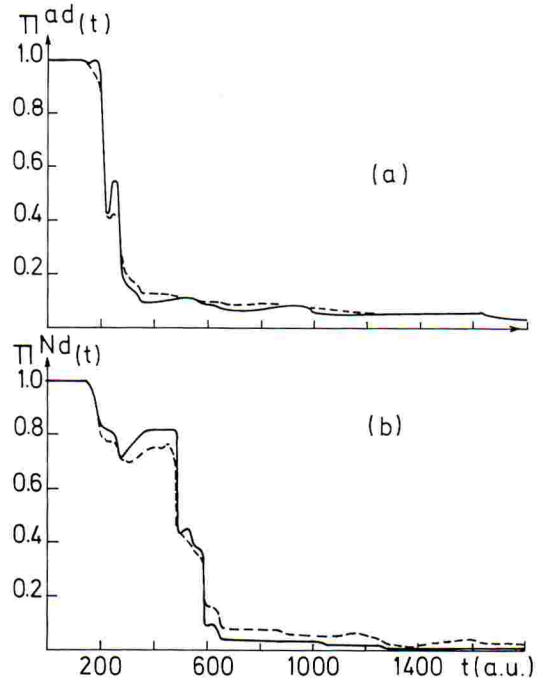

Fig. 4. Probability functions of remaining on the potential energy surface studied, calculated with frozen $\mathbf{B}_k$ matrices. Full line: $b = 1$; dashed line: $b = 2$. (a) $\Pi^{ad}(t)$; (b) $\Pi^{Nd}(t)$.

figs. 3 and 4, the results are very similar except a slight difference in $C(t)$ for the diabatic case, in the integral $1400 \lesssim t \lesssim 1800$ au.

9.2. *Influence of the freezing of* **B**

The comparison is not made in the canonic diabatic case. As a matter of fact, if the Gaussians move on this state (which is harmonic) and if $b = 1$, the Gaussians' widths remain unchanged. Thus, the comparison is useless for $b = 1$. Furthermore, the calculation was not done for $b = 2$ with **B** frozen.

9.2.1. $b = 1$

The functions $C^{ad}(t)$ (figs. 1 and 3, full lines) as well as $\Pi^{ad}(t)$ (figs. 2 and 4, full lines) present similar global features. However, the relative heights of the recurrences in $C(t)$ are different and furthermore the second recurrence presents a splitting in the case where **B** varies as a function of time.

The decreasing laws of the functions $\Pi(t)$ are very similar but the curve has a more oscillatory behavior if **B** is not kept frozen.

9.2.2. $b = 2$

As far as $C(t)$ is concerned (see figs. 1 and 3, dashed lines), the difference between the cases where **B** is frozen or not is more important for $b = 2$ than for $b = 1$. The relative heights are similar but their absolute values are nearly twice or three times greater when **B** varies. Furthermore, in the diabatic case, the recurrence at $t \approx 1000$ au is split when **B** is not kept constant.

The functions $\Pi(t)$ (figs. 2 and 4, dashed lines) decrease with comparable rates but the detailed features are rather different in the diabatic case since $\Pi(t)$ presents several peaks when **B** is free to vary.

9.3. *Comparison with Köppel's results*

9.3.1. $C^{ad}(t)$

The shapes of the peaks are different in the sense that they are rather well separated from each other in the calculated function of this work whereas the function obtained by Köppel is smoother (fig. 5). Nevertheless, the positions of the recurrences are similar to what Köppel obtained in the full $C(t)$ and their intensities are of the same order. However, if the gross features are reproduced, the details are different. This is probably due to the very small basis employed in this work (see section 10).

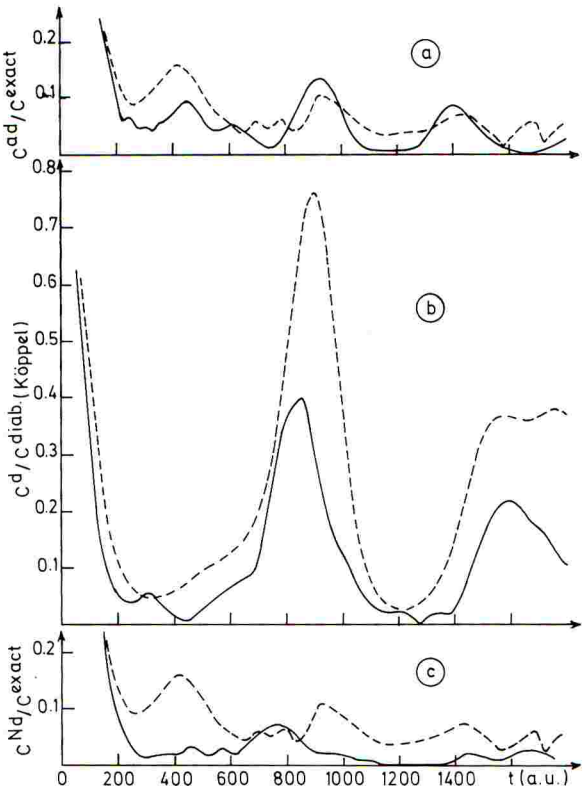

Fig. 5. Comparison with Köppel's correlation functions. Full line: our results – dashed line: Köppel's functions. (a) Our C^{ad}/Köppel's exact $C(t)$; (b) our $C^{d}(t)$/Köppel's diabatic $C(t)$; (c) our $C^{Nd}(t)$/Köppel's exact $C(t)$.

9.3.2. $C^{d}(t)$

The shapes and the positions of the recurrences are very similar to those obtained by Köppel for his diabatic correlation function (fig. 5). However, the heights are quite different. They do not oscillate but rather decrease regularly. This is due to the fact that each Gaussian is weighted by the square root of the probability of remaining on the surface. This decaying factor is absent in the pro-

cedure used by Köppel since he took the coupling constant λ equal to zero.

9.3.3. $C^{Nd}(t)$

The recurrences at $t \approx 750$, $t \approx 1450$ and $t \approx 1670$ au may contribute to those which appear in the full exact correlation function obtained by Köppel but after $t \approx 2000$ au, the function becomes too small for any comparison to be made.

9.3.4. Total C(t)

In the construction of the total correlation function, the diabatic component which has to be considered must not be the canonic one $C^{d}(t)$ but rather $C^{Nd}(t)$, for which the initial conditions start on a dynamically meaningful potential energy surface.

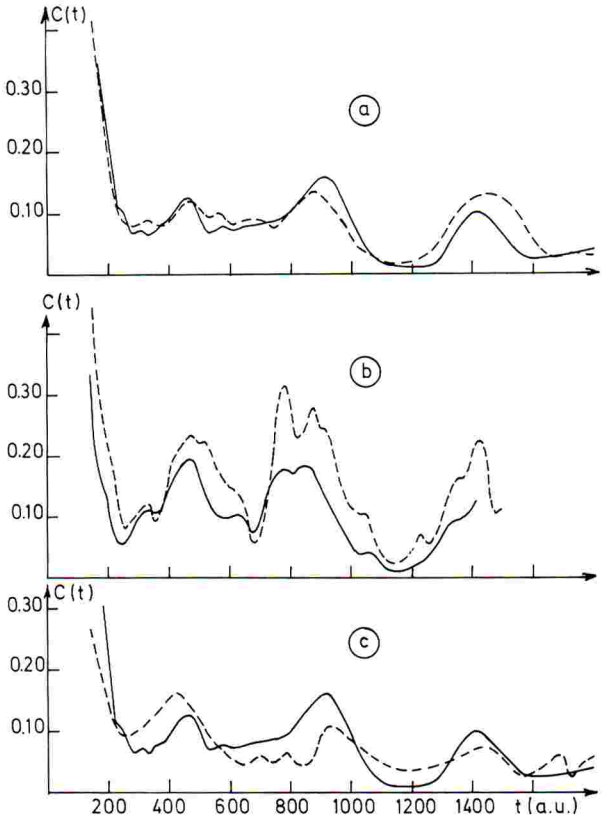

Fig. 6. Total autocorrelation function $C(t) = C^{ad}(t) + C^{Nd}(t)$. Full line: $b = 1$; dashed line: $b = 2$. (a) $\mathbf{B}_k$ frozen; (b) $\mathbf{B}_k$ variable; (c) dashed line: Köppel's exact $C(t)$, full line: our result with $\mathbf{B}_k$ frozen $= \mathbf{1}$.

The total functions

$$C(t) = C^{ad}(t) + C^{Nd}(t)$$

are presented in fig. 6. When **B** is kept constant (figs. 6a, 6c), the gross features are qualitatively reproduced but the recurrences are too high, except the first one which is too small. In the case where **B** is free to vary (fig. 6b), the heights of all the recurrences are too big and their shapes are rather different from those obtained by Köppel in particular for $b = 2$. Though not very good, the qualitative agreement is better with $b = 1$.

9.3.5. The probability $\Pi^{d}(t)$

Since Köppel presented the probability $P_2(t)$ of remaining on the upper canonic diabatic state, only the function $\Pi^{d}(t)$ of this work (fig. 2b) has to be compared with $P_2(t)$. The first minimum of $P_2(t)$ occurs near $t = 850$ au and the first maximum near $t = 1250$ au. Neither for $b = 1$ nor for $b = 2$ does one obtain any maximum in $\Pi^{d}(t)$ if one excepts the damped oscillations. This is obviously due to the fact that the contribution back from the $\tilde{X}$ state is dropped. As a matter of fact, the wave packet is considered as moving on a single surface and the reversibility of the process is not reproduced.

10. Discussion

10.1. The effect of the basis

As was briefly said in section 9, a parallel can be made between $C^{d}(t)$ and Köppel's diabatic correlation function on one hand, and between our total $C(t)$ and Köppel's exact correlation function on the other hand. However, the agreement stands only at a qualitative level. Since the study covers only the short-time range ($t \approx 1000$ au) (for which that part of the wave packet constituted by cross terms of the type $p_k(t_1)[1 - p_i(t_2)]$ can be considered as negligible), this is probably due to the smallness of the basis set. This argument is supported by the fact that the results are better for $b = 1$ than for $b = 2$. Furthermore, a calculation was done for $b = 3$ and for

which **B** was allowed to vary, in the canonic diabatic case. The result was dramatic: even though the wavefunction was normalized at each time step, the correlation function reached the value of ≈ 1.3 for $t \approx 75$ au. This is typically an effect of the incompleteness of the basis [18].

10.2. The decreasing law of the functions $\Pi(t)$

All the calculated functions $\Pi(t)$ decrease more or less regularly without exhibiting those large oscillations obtained by Köppel [10]. As pointed out above (section 9.3.5), only one part of the nondiabatic process is studied, that related to the motion of that portion of the wave packet which remains on the only investigated potential energy surface. This portion becomes smaller and smaller as the wave packet moves back and forth through the coupling region. The recurrences coming from the complementary portion of the wave packet are not calculated in this work. This explains why the functions $\Pi(t)$ decay much too fast.

10.3. Criterion for the choice of the diabatic basis set

In principle, the study of the nonadiabatic process can be made with the adiabatic or the diabatic basis set, as far as the latter can be derived [19]. In the adiabatic/diabatic model of this paper, defined by Köppel [10], it is obvious that the canonic diabatic basis set is inadequate to describe the phenomenon (see fig. 5 and section 9.3). The reason is that the canonic diabatic potential energy surface has nothing to do with the only physically acceptable adiabatic potential energy surface in the Franck–Condon zone which lies outside the coupling region. As a matter of fact, as far as the nuclei's motions are concerned, the importance of the choice of adequate potential energy surfaces is clear since the forces between them are unequivocally defined [20]. This is the justification for the choice of the Nikitin diabatic potential energy surfaces used to calculated the correlation function $C^{Nd}(t)$. This basis set seems to give qualitatively good results if one keeps in mind the effect of the incompleteness of the Gaussian basis set employed.

10.4. Adiabatic / diabatic behavior

When one looks at $\Pi^{ad}(t)$ and $\Pi^{Nd}(t)$ (or $\Pi^{d}(t)$), one could be very surprised that they all decrease till very small values. The expected result should be either great values of $\Pi^{ad}(t)$ and small ones for $\Pi^{Nd}(t)$ or vice versa, i.e. either the system essentially behaves adiabatically or diabatically. This is undoubtedly not the case. The explanation of this unexpected result can be found in the nuclear motions taking place on each potential energy surface and in particular in the average absolute value of the antisymmetric coordinate when the transition takes place, i.e. $|\overline{Q_u}|_{tr}$, since it plays the role of an impact parameter to the apex of the conical intersection [4] (section 7). The analysis of the trajectories gives the values of $|\overline{Q_u}|_{tr}$ reported in table 1. In the adiabatic motion, the wave packet becomes rather thin near the intersection whereas in the diabatic motion, it is not true: either it remains unchanged (harmonic case of the canonic diabatic surface) or it spreads. This behavior can be understood via the coupling element H_{12}, function of Q_u only, and the distribution of the initial conditions of the trajectories. Since H_{12} is a function of Q_u only, the upper adiabatic potential energy surface is steeper along Q_u than the canonic diabatic one, which brings about a sort of aspiration of the wave packet towards the apex of the cone, some kind of a "black hole" effect. The difference between the adiabatic and canonic diabatic wave packet's behavior depends of course on the parameter λ (eq. (3.2)): the larger λ the larger the difference between the adiabatic and diabatic behavior. As far as the difference between the two diabatic (canonic and Nikitin) motions is concerned, this is a question of distribution of the initial conditions onto the potential energy surface. The initial wave packet, i.e. the initial conditions of the trajectories, is the same for both cases. However, as the Nikitin diabatic surface coincides with the adiabatic one, it is steeper along Q_u than the canonic diabatic surface. Thus, the mean potential energy in Q_u is greater for the motion on the Nikitin diabatic surface when the wave packet arrives in the coupling region, which leads to the spreading observed in this zone, and thus to a smaller prob-

Table 1
Averaged absolute value of the antisymmetric coordinate $|\overline{Q_u}|_{tr}$ when the transition takes place

Adiabatic case	Canonic diabatic case	Nikitin diabatic case
≈ 0.2	≈ 0.8	≈ 1.2

ability of remaining on that surface. The fact that the recurrences in $C(t)$ essentially come from the adiabatic component $C^{ad}(t)$ can also be linked to the difference between the motions on the two types of potential energy surfaces. On the Nikitin diabatic surface, it seems that the spreading of the wave packet leads to a worse recurrence back in the Franck–Condon region and then to a smaller overlap with the initial wave packet.

In the case of the conical intersection of $C_2H_4^+$ studied in this work, it is obvious that one cannot say that the behavior of the system is essentially diabatic or adiabatic. The interaction between the two states (either diabatic or adiabatic) cannot be considered as a perturbation, as could be said for H_2O^+ [4] which behaves essentially diabatically. Here, the process is both adiabatic and diabatic and the two contributions are to be taken into account if one wants to understand the complexity of the spectrum [10]. Furthermore, in the case of $C_2H_4^+$, the crossed terms (i.e. those for which the motion is sometimes adiabatic and sometimes diabatic) are undoubtedly very important at long time range since both $\Pi^{ad}(t)$ and $\Pi^{Nd}(t)$ become very small when t increases.

Acknowledgement

I am very grateful to Professor J.C. Lorquet for the stimulating discussions we had. I would like to thank Professor H. Köppel for providing me with his data on the exact and diabatic correlation functions and on the probability $P_2(t)$. This work has been supported by the Belgian government (Action de Recherche Concertée) and the "Fonds de la Recherche Fondamentale Collective".

Appendix

The fact that, at time t, the Gaussians are not characterized any longer by the same $\mathbf{B}_k$ is equivalent to saying that the basis vectors have rotated independently in such a way that the new reference frame is not only the old one which would have been translated and rotated. Thus, the expansion coefficients c_k must be adapted to this new basis. One way to do this is to determine the c_k by a variational procedure. However, we proceeded in another manner. Each Gaussian function is considered with its initial center but with its $\mathbf{B}_k$ matrix at time t:

$$G_k^{(t)}(\boldsymbol{Q}, 0) = \exp\Big\{ -\tfrac{1}{2}\big[\boldsymbol{Q} - \boldsymbol{Q}_k(0)\big]^{\mathrm{T}} \cdot \mathbf{B}_k^{(t)} \big[\boldsymbol{Q} - \boldsymbol{Q}_k(0)\big] + \mathrm{i}\hbar^{-1} \boldsymbol{P}_k^{\mathrm{T}}(0) \cdot \big[\boldsymbol{Q} - \boldsymbol{Q}_k(0)\big] \Big\}. \quad (A.1)$$

This new basis set is diagonalized [4,6] and $M(t) \leqslant N$ linearly independent orthogonal functions $F_j^{(t)}(\boldsymbol{Q}, 0)$ (for which the norm s_j is greater than a fixed value) are used to represent the wavefunction:

$$\Psi(\boldsymbol{Q}, 0) = \sum_j^{M(t)} u_j^{(t)} F_j^{(t)}(\boldsymbol{Q}, 0), \quad (A.2)$$

$$u_j^{(t)} = s_j^{-1} \iiint \mathrm{d}\boldsymbol{Q}\ \Psi(\boldsymbol{Q}, 0) F_j^{(t)}(\boldsymbol{Q}, 0). \quad (A.3)$$

The final step is then the same as that exposed in ref. [4] to obtain the c_k.

References

[1] S. Shi, J. Chem. Phys. 79 (1983) 1343; 81 (1984) 1794; R.T. Skodje and D.G. Truhlar, J. Chem. Phys. 80 (1984) 3123.
[2] E.J. Heller, J. Chem. Phys. 65 (1976) 4979.
[3] E.J. Heller, J. Chem. Phys. 62 (1975) 1544; S.Y. Lee and E.J. Heller, J. Chem. Phys. 76 (1982) 3035; G. Drolshagen and E.J. Heller, J. Chem. Phys. 82 (1985) 226.
[4] D. Dehareng, Chem. Phys. 110 (1986) 375.
[5] E.J. Heller, E.B. Stechel and M.J. Davis, J. Chem. Phys. 73 (1980) 4720; R.L. Sundberg and E.J. Heller, Chem. Phys. Letters 93 (1982) 586.

[6] M.J. Davis and E.J. Heller, J. Chem. Phys. 71 (1979) 3383.
[7] N. De Leon and E.J. Heller, J. Chem. Phys. 78 (1983) 4005;
N. De Leon, M.J. Davis and E.J. Heller, J. Chem. Phys. 80 (1984) 794.
[8] E.E. Nikitin, Theory of elementary atomic and molecular processes in gases (Clarendon Press, Oxford, 1974);
E.E. Nikitin and L. Zülicke, Selected topics of the theory of chemical elementary processes (Springer, Berlin, 1978);
M. Desouter-Lecomte, C. Galloy, J.C. Lorquet and M. Vaz Pires, J. Chem. Phys. 71 (1979) 3661;
D. Dehareng, X. Chapuisat, J.C. Lorquet, C. Galloy and G. Raseev, J. Chem. Phys. 78 (1983) 1246.
[9] H. Köppel, W. Domcke and L.S. Cederbaum, Advan. Chem. Phys. 57 (1984) 59.
[10] H. Köppel, Chem. Phys. 77 (1983) 359.
[11] E. Wigner, Phys. Rev. 40 (1932) 749;
E.J. Heller, J. Chem. Phys. 65 (1976) 1289; 68 (1978) 2066;
F. Fiquet-Fayard, M. Sizun and S. Goursaud, J. Phys. (Paris) 33 (1972) 669.
[12] H.F. Harmuth, J. Math. Phys. 36 (1957) 269;
J. Mazur and R.J. Rubin, J. Chem. Phys. 31 (1959) 1395;
E.A. McCullough and R.E. Wyatt, J. Chem. Phys. 54 (1971) 3578;
K.C. Kulander, J. Chem. Phys. 69 (1978) 5064;
A. Askar and A.S. Cakmak, J. Chem. Phys. 68 (1978) 2794;
P.M. Agrawal and L.M. Raff, J. Chem. Phys. 74 (1981) 5076.
[13] H.D. Meyer, Chem. Phys. 61 (1981) 365;
R.D. Coalson and M. Karplus, Chem. Phys. Letters 90 (1982) 301;
S.Y. Lee, Chem. Phys. 108 (1986) 451.
[14] E.J. Heller, J. Chem. Phys. 75 (1981) 2923.
[15] K.C. Kulander and E.J. Heller, J. Chem. Phys. 69 (1978) 2439;
D.J. Tannor and E.J. Heller, J. Chem. Phys. 77 (1982) 202;
R.T. Skodje, Chem. Phys. Letters 109 (1984) 227.
[16] M.F. Herman, J. Chem. Phys. 85 (1986) 2069.
[17] C.W. Gear, Numerical initial value problems in ordinary differential equations (Prentice Hall, Englewood Cliffs, 1971).
[18] M.F. Herman and E. Kluk, Chem. Phys. 91 (1984) 27.
[19] A.D. McLachlan, Mol. Phys. 4 (1961) 417;
M. Baer, Chem. Phys. Letters 35 (1975) 112; Chem. Phys. 15 (1976) 49;
C.A. Mead and D.G. Truhlar, J. Chem. Phys. 77 (1982) 6090;
M. Desouter-Lecomte, D. Dehareng and J.C. Lorquet, J. Chem. Phys. 86 (1987) 1429.
[20] G.G. Hall, Intern. J. Quantum Chem. 31 (1987) 383.